XIX IMEKO World Congress
Fundamental and Applied Metrology
September 6–11, 2009, Lisbon, Portugal

ANALYSIS AND DESIGN OF INDUCTIVE BIOSENSORS FOR MAGNETIC IMMUNO ASSAY

Bruno Andò[1], Salvatore Baglio[1], Angela Beninato[1], Giorgio Fallica[2], Vincenzo Marletta[1], Nicola Pitrone[1]

[1] DIEES, University of Catania, Catania, Italy, salvatore.baglio@diees.unict.it
[2] STMicroelectronics, Catania, giorgio.fallica@st.com

Abstract – In this paper an inductive integrated sensor for biomedical applications is investigated through analytical models and numerical simulations such to obtain an optimized device design. This biosensor addressed here is based on the use of magnetic particles that suitably coated act as markers of the bio-molecule to be detected. The sensing principle of the device is related to the magnetic field thickening determined by the presence of magnetic particles in the active device area. An accurate finite element numerical simulation is therefore necessary to optimize the sensor performances; simulations have been performed by representing the magnetic particles with an equivalent volume having the same magnetic properties. The simulations have allowed analysing the influence of the different device parameters on the sensor response. An optimized design procedure has been therefore sketched and the results are reported in this paper.

Keywords: inductive sensors, FEM, magnetic particles.

1. INTRODUCTION

This work reports the study, the simulations, the optimization and the design of a inductive-based device to be fabricated in a dedicated Si microtechnology that is aimed for immune-bio-sensing applications.

The growing demand for biosensors with very high sensitivity and specificity, with short analysis time, low cost, easy to handle, able for portable applications is the motivation of this work. A device with these characteristics is important for applications in different fields like public health, clinical analysis, water and air pollution, biotechnology.

High sensitivity and specificity can be obtained by using Immunological techniques [1-2], which are based on the biological recognition of the analyte to be detected by specific antigen or antibodies.

Detection is made by coupling these molecules to suitable markers, such as radioactive compounds, enzymes, fluorophores and luminescence ones. In front of these, magnetic markers have potential advantages, which are related to their low price, very high stability and absence of toxicity. In addition, biomolecules fixed to magnetic nanoparticles can be easily localised and manipulated by suitable magnetic fields [2-4]. The problem of detecting biological agents is therefore shifted to the ability of sensing the presence of a small number of magnetic particles.

In many works [5-8] inductive devices have been realized: these sensors are based on the change of the inductance of a coil as a result of the presence of a certain density of magnetic particles in the active region of the sensor device. Both this region and the magnetic particles must be functionalized with a antibody specific to the analyte to be detected. The interaction antibody-analyte-antibody bonds the magnetic particles to the sensors surface, which leads to a change of magnetic flux in the device and, hence, of the inductive impedance. In comparison with other kinds of magnetic biosensors, inductive devices have several potential advantages, which are related to their higher simplicity, fully compatibility with standard Si technology materials, low cost and higher flexibility.

2. DEVICE SIMULATION AND DESIGN

The device presented here is based on a planar coreless differential transformer configuration. A primary coil generates a magnetic flux which links with two secondary coils, with opposite winding sense, connected in a differential arrangement. The primary coil generates a magnetic flux that induces voltages with equal values but opposite in sign in the secondary coils, due to their opposite winding sense; therefore the resulting output voltage, which is the difference between the voltages across the secondary coils, is zero when no magnetic particles are present. On the other hand, the presence of magnetic particles in one of the secondary coils will cause a redistribution of the magnetic flux lines, which will result denser near the magnetic particles, therefore resulting in a non-zero differential output voltage. This working principle is schematized in Fig. 1.

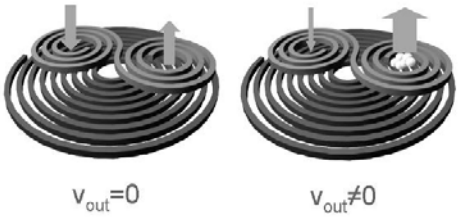

Fig. 1. Working principle of the planar differential transformer.

In this approach one of the secondary coils acts as the "active" sensor, while the other one acts as "dummy", like in most differential sensing approaches. In particular here the differential configuration is used not to enhance sensitivity; in fact there are no opposite variations of inductance, but to lower the noise floor.

The primary coil is a source of excitation of the sensor. This approach allows a more flexible optimization of the device in terms of sensitivity, in fact in the case of the transformer the open circuit voltage at the secondary coil, if expressed in terms of the current applied to the primary winding, is proportional to the product of the number of turns of the primary and the secondary coils as reported in Equation (1).

$$S = N_1 N_2 \frac{2\Re_1 + \Re_2}{\left[\Re_1\left(2 - \frac{\Delta L}{L_2^{'}}\right) + \Re_2\left(1 - \frac{\Delta L}{L_2^{'}}\right)\right]^2} \frac{di_1}{dt} \qquad (1)$$

Where

- N_1 and N_2 are the number of turns respectively of the primary and each secondary coils.
- $\Re_1$ and $\Re_2$ are the reluctances of primary and secondary coils.
- $i_1$is the current in the primary coil.
- ΔL is the difference of inductance of the secondary coil over which the magnetic beads are; such variation is due to the thickening of magnetic field.
- L'_2 is the inductance value of the secondary coil over which the magnetic beads are.

While the secondary coils can be subjected to more restrictive design constraints due to their sensing function, the primary coils has less restrictions, therefore both the sensitivity requirements and the design constraints can be more easily satisfied with respect to the single inductor case, by proper designing the primary and secondary coils.

Furthermore, the approach presented here is intrinsically differential, thus allowing a better rejection of noise and interferences. It is suitable for the integration in Si technology due to its simple and planar geometry.

Moreover, it is not based on the direct estimation of the inductance, resulting in a great simplification of the measurement strategy. In fact the magnetic particles act as a moveable nucleus and the differential output voltage at the secondary coils is directly related to the number (or density) of magnetic particles. Therefore a high impedance detection of the differential output voltage at the secondary coils is a simple but good strategy to the detection of the magnetic particles.

The simulated differential transformer is made up of two metal layers (Metal1 and Metal2) separated by a layer of silicon oxide. The primary winding has been realized in the Metal 1 layer, while the Metal 2 has been used to realize the secondary windings. A passivation layer covers the whole transformer. Fig. 2 shows a schematics of the cross section of the device: the primary and secondary centers are indicated by vertical axis.

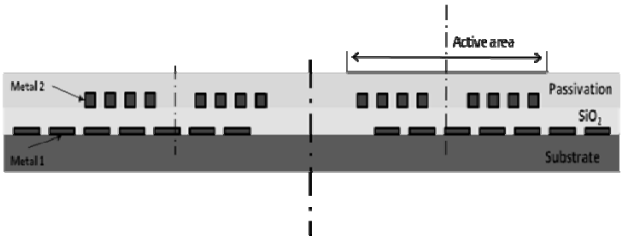

Fig. 2. Schematic of the cross-section along a radial direction.

The geometric characteristics of the different layers are summarized in Table1.

Table 1. Geometric characteristics of differential transformer.

Metal 1 thickness	0.5 µm
Minimum track spacing and width for Metal1	1 µm
Oxide thickness	1 µm
Metal2 thickness	1 µm
Minimum track spacing and width for Metal2	1.2 µm
Passivation thickness	0.5 µm

The planar transformer has been studied with the finite element software ANSYS®. We have simulated the presence of Spherotech® CM-10-10 magnetic beads with the characteristics shown in Table 2. and Fig. 3.

Table 2. Characteristics of Spherotech CM 10-10 magnetic beads.

Diameter	1 µm
%Iron	12%
Magnetic saturation	Ms=0,46 [T]
Susceptibility	X=11.3

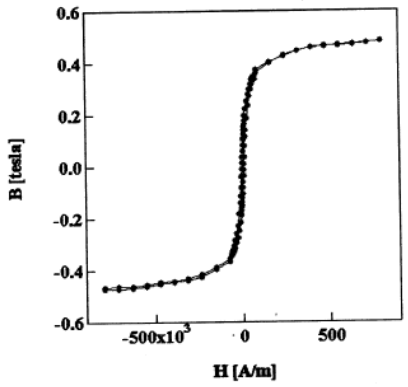

Fig. 3. B-H curve for Spherotech CM 10-10 magnetic beads.

The presence of a certain density of magnetic particles is modeled both assuming a continuous layer with a equivalent volume and symbolizing these particles by cylindrical volumes: the same distribution of magnetic field and results

are obtained; for simplicity we have adopted a continuous layer (with the same magnetic permeability and with an equivalent volume) whose centre is coincident with the active secondary one.

The magnetic beads in the sensing area of the active secondary coil attract the magnetic flux lines and change the magnetic field distribution by creating a thickening zone, as shown in Fig. 4.

Simulations have been performed to determine the influence of the different device parameters (as number of rings, separation between rings, active surface dimension, position of secondary centre, etc) on the sensor response. This is described by ΔΦ (change of concatenated flux as result of the presence of the magnetic particles).

Fig. 4. Distribution of the magnetic field produced by the primary coil and view of the secondary coils (top). Zoom of the area inside the active coil (the one at the right in the top figure) both in absence (bottom-left) and in presence (bottom-right) of magnetic beads.

To establish the ideal position of the secondary compared to the primary coil, an arbitrary geometry is chosen: we have considered a primary coil with 9μm internal radius, 13 rings and lowest spacing and track; a secondary coil with 5 rings and lowest spacing and track, a source current of 2 mA per μm and a fixed amount of magnetic particles. The simulation of the device response as function of the secondary position (that is the centre of magnetic cylinder) indicates the presence of an optimal distance from the primary coil centre (see Fig. 5).

After fixing the secondary coil position, we have investigated about the track spacing of primary coil; we have obtained that when the ring width changes, the minimum value of track separation technologically available is always the better, as shown in Fig. 6

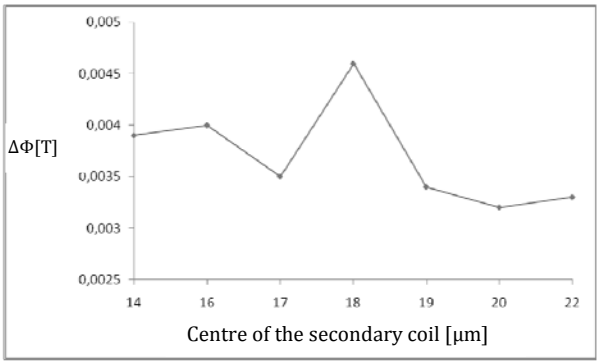

Fig. 5. Optimal position of secondary coil and magnetic cylinder.

To establish the track width of primary coil we fixed the spacing to the value of 1μm and we changed the track width from 1μm to 8μm. The output increases with the width. The ring number of primary coil must be chosen as function both ΔΦ and final device dimension.

An important feature in the realization of the integrated device is related to the current value in the primary coil. This current will be therefore taken as the largest acceptable value for the wiring width that doesn't induce thermal effects.

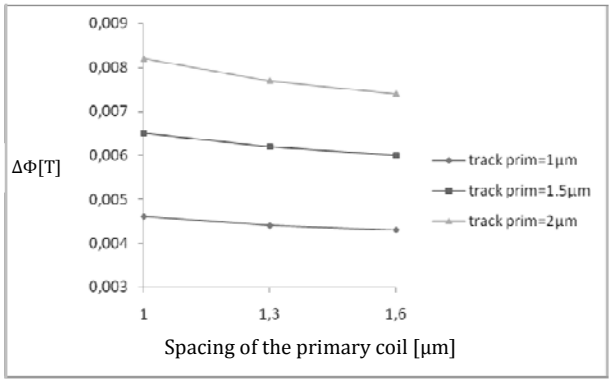

Fig. 6. ΔΦ versus spacing of primary coil.

In Fig. 7 the simulation of the response as function of the number of rings in the primary coil is plotted.

In accordance with Equation (1), the device output increases with the number of primary turns. As for the track width, the number of rings must be chosen also in function of the final dimension.

To evaluate the smallest amount of magnetic particles that we can detect, a simulation in function of the radius of the magnetic layer has been performed.

It was considered a secondary coil with a inner radius of 3μm: we have obtained that the minimum radius must be comparable with the size of the inner radius of the secondary coil. Indeed, as shown in Fig. 8, a magnetic layer with a 1μm radius is not detected, while the flux change for a layer with 3μm is small but detectable. For a larger magnetic layer there is a greater output because the amount of magnetic field attracted is bigger.

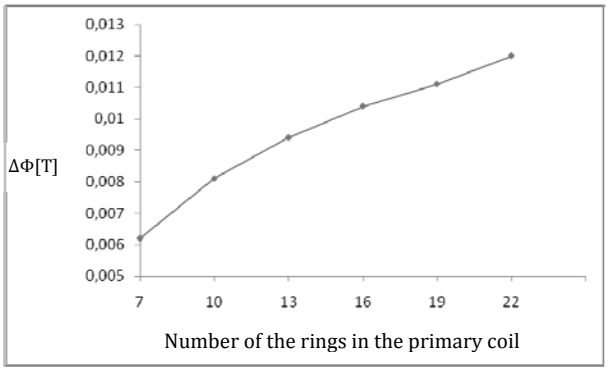

Fig. 7. Simulation of the device response as function of number of the turn in primary coil.

To define the secondary coil dimension we simulated the device response as function of the size of the cut area of the active secondary coil, with a 11.4µm radius of magnetic layer. The ratio between the radius of magnetic cylinder and the radius of the ideal cut area (the maximum point in Fig. 9) is 1.2.

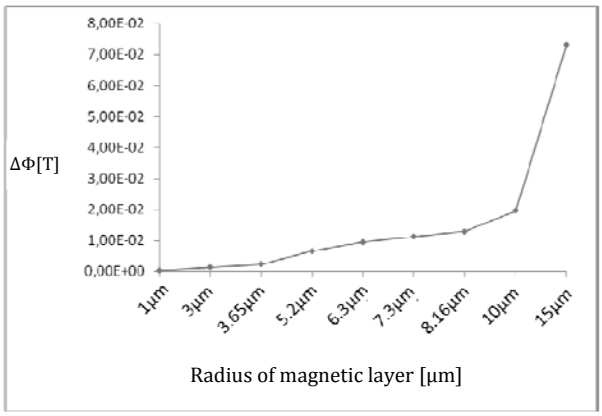

Fig. 8 Dependence of the device response on the radius of magnetic layer.

To define the number of the turns of the secondary coil we use Equation (1) after we have established the cut area of active coil: because the output increase whit the number of the ring of the secondary coil, it is convenient to create a secondary as dense as possible, with the minimum track spacing and width.

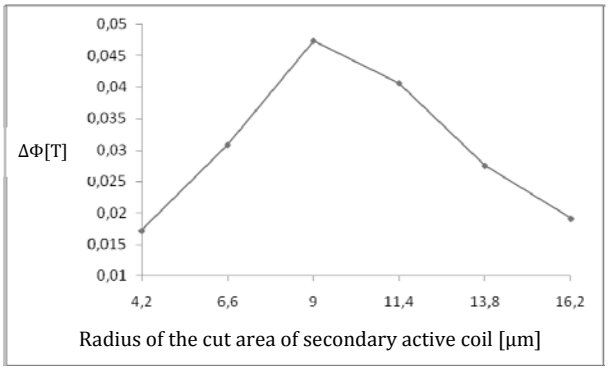

Fig. 9. ΔΦ versus radius of the cut area.

According to all these simulations, the device has been designed using, for both primary and secondary coils, the smallest separation technologically available between the metal tracks (1µm for the primary coil and 1.2µm for the secondary one), a track width of 2.5µm for primary coil and 1.2µm for the secondary coil.

Taking into account the above described optimization criteria and considering the design specifications as given in Table 3 as starting points, an integrated inductive device for biomedical applications have been designed.

Table 3. Desired sensor performances

Equivalent volume of magnetic particles to be detected	28.27 µm^3
Total device dimension	12100-13225 µm^2

The results obtained are reported in Table 4.

3. CONCLUSIONS

In this paper we have reported the study, simulation and optimized design of a planar differential transformer made up two metal layer with a separation of oxide.

This device is the core section for an integrated magnetic immune-sensor.

Simulations have been performed to determine the influence of the different device parameters (as number of rings, separation between rings, active surface dimension, position of secondary centre, etc) on the sensor response. This is described by ΔΦ (change of concatenated flux as result of the presence of the magnetic particles).

The integrated sensor fabrication is in progress and the device experimental characterization will be performed by mechanically placing the magnetic beads on the sensor surface. Future work will address the sensor surface coating to fix the magnetic particles and to realize the antibody-antigene selective mechanism.

Table 4. Optimized inductive microsensor parameters.

Primary coil	Turns number = 13 Track width = 2.5 µm Spacing = 1 µm Inner radius = 9 µm
Secondary coils	Turns number = 5 Track width = 1.2 µm Spacing = 1.2 µm Inner radius ≤ 3 µm Centers positions=±18 µm
Radius of the ideal cut area	3.6 µm
Current in the primary coil	2 mA/µm

REFERENCES

[1] K. Larsson, K. Kriz, D. Kriz, "Magnetic Transducers in and Bioassays", *Analusis* 1999, 27 N 7, 617-621.vol.13, 1998,

[2] K. Kriz, J. Gehrke, and D. Kriz, "Advance toward magneto immunoassays", *Biosensors & Bioelec.*, vol.13, 1998, pp.817

[3] D.R.Baselt, G.U.Lee, K.M.Handen, L.A.Chrisey and R.J.Colton, "a High-sensitivity Micromachined Biosensor" *Proc. Of the IEEE*, vol. 85, 1997. pp672

[4] R.L.Edelstein, C.R.Tamanaha, P.E.Sheehan, M.M.Miller, D.R.Baselt, L.J.Whitman and R.J.Colton, "The BARC biosensor applied to the detection of biological warfare agents", *Biosensors & Bioelectronics*, vol. 14, 2000, pp805

[5] S. Baglio, S. Castorina, . N. Savalli, "Integrated inductive sensors for magnetic immuno assay applications", *IEEE Sensors Journal*, Vol. 5, Issue 3, June 2005 pp.372 – 384

[6] C. Serre, S. Martìnez, A.Pérez-Rodrìguez, J.R. Morante, J.Esteve, J.Montserrat, "Si technology based microinductive devices for biodetection applications", *Sensors and Actuators* A 132 (2006) pp499-505

[7] S.M. Azimi, M.R. Bahmanyar, M.Zolgharni, and W.Balachandran, "An Inductance-based Sensor for DNA Hybridization Detection", *Proc. of the 2nd IEEE International Conference on Nano/Micro Engineered and Molecular Systems January* 16 - 19, 2007

[8] A. Vilà, A. Romano-Rodrìguez, F. Hernàndez, S. Martìnez, C. Serre, A. Pèrez-Rodrìguez, J.R. Morante, "Microcoils for biosensors fabricated by focused ion beam (FIB)", *Electron Devices,* 2005, pp. 209-212

[9] Spherotech, Inc., http://www.spherotech.com